P. Netherwood

BRL MR 2760

BRL

AD

MEMORANDUM REPORT NO. 2760

TENSILE STRESS-STRAIN CURVES--III, ROLLED HOMOGENEOUS ARMOR AT A STRAIN RATE OF 0.42 S^{-1}

Ralph F. Benck
Joseph L. Robitaille

June 1977

Approved for public release; distribution unlimited.

USA ARMAMENT RESEARCH AND DEVELOPMENT COMMAND
USA BALLISTIC RESEARCH LABORATORY
ABERDEEN PROVING GROUND, MARYLAND

Destroy this report when it is no longer needed.
Do not return it to the originator.

Secondary distribution of this report by originating or sponsoring activity is prohibited.

Additional copies of this report may be obtained from the National Technical Information Service, U.S. Department of Commerce, Springfield, Virginia 22151.

The findings in this report are not to be construed as an official Department of the Army position, unless so designated by other authorized documents.

The use of trade names or manufacturers' names in this report does not constitute indorsement of any commercial product.

REPORT DOCUMENTATION PAGE

READ INSTRUCTIONS BEFORE COMPLETING FORM

1. REPORT NUMBER: MEMORANDUM REPORT NO. 2760
2. GOVT ACCESSION NO.:
3. RECIPIENT'S CATALOG NUMBER:

4. TITLE (and Subtitle): Tensile Stress-Strain Curves--III, Rolled Homogeneous Armor at a Strain Rate of 0.42 S^{-1}
5. TYPE OF REPORT & PERIOD COVERED: Final
6. PERFORMING ORG. REPORT NUMBER:

7. AUTHOR(s): Ralph F. Benck, Joseph L. Robitaille
8. CONTRACT OR GRANT NUMBER(s):

9. PERFORMING ORGANIZATION NAME AND ADDRESS: USA Ballistic Research Laboratory, Aberdeen Proving Ground, MD 21005
10. PROGRAM ELEMENT, PROJECT, TASK AREA & WORK UNIT NUMBERS: RDT&E Proj. No. 1W161102AH43

11. CONTROLLING OFFICE NAME AND ADDRESS: USA Materiel Development & Readiness Command, 5001 Eisenhower Avenue, Alexandria, VA 22333
12. REPORT DATE: JUNE 1977
13. NUMBER OF PAGES: 34

14. MONITORING AGENCY NAME & ADDRESS (if different from Controlling Office):
15. SECURITY CLASS. (of this report): Unclassified
15a. DECLASSIFICATION/DOWNGRADING SCHEDULE:

16. DISTRIBUTION STATEMENT (of this Report)

Approved for public release; distribution unlimited.

17. DISTRIBUTION STATEMENT (of the abstract entered in Block 20, if different from Report)

18. SUPPLEMENTARY NOTES

19. KEY WORDS (Continue on reverse side if necessary and identify by block number)

armor
steel
penetrators
strain-rate effects

20. ABSTRACT (Continue on reverse side if necessary and identify by block number) bet/2972

This report presents the results of tensile tests at a strain rate of 0.42 s^{-1} for 38mm and 100mm thick rolled homogeneous armor. Young's modulus, Poisson's ratio, yield and ultimate strengths are reported for tests performed at 23°C.

TABLE OF CONTENTS

LIST OF ILLUSTRATIONS

LIST OF TABLES

I. INTRODUCTION

The tests herein were conducted as part of a continuing[1-7] effort of the Solid Mechanics Branch of the Terminal Effects Division to characterize the material properties of armor and armor penetrators. The data can be used in the design of armored vehicles and projectiles, and as input for computer codes modeling penetration processes.

This report presents the results of tensile tests at strain rates of 0.42 s^{-1} for samples from 38mm and 100mm thick plates of rolled homogeneous armor (RHA). Specimens for this study were obtained from planes of the plate parallel to the rolled direction. The results include the modulus of elasticity, Poisson's ratio, yield and ultimate tensile strengths and engineering stress-strain curves. Stress-strain curves made at strain rates of 3×10^{-4} s^{-1} and alpha phase Hugoniot studies of the same batch of RHA are reported elsewhere.[7,8]

---

[1] *E. A. Murray, Jr. and J. H. Suckling, "Quasi-Static Compression Stress-Strain Curves--I, Data Gathering and Reduction Procedures; Results for 1066 Steel", BRL Memorandum Report No. 2399, Ballistic Research Laboratory, Aberdeen Proving Ground, MD, January 1974. AD# 922704L.*

[2] *E. A. Murray, Jr., "Quasi-Static Compression Stress-Strain Curves--II, 7039-T64 Aluminum", BRL Memorandum Report No. 2589, Ballistic Research Laboratory, Aberdeen Proving Ground, MD, February 1976. AD #B009646L*

[3] *R. F. Benck and E. A. Murray, Jr., "Quasi-Static Compression Stress-Strain Curves--III, 5083-H131 Aluminum", BRL Memorandum Report No. 2480, Ballistic Research Laboratory, Aberdeen Proving Ground, MD, May 1975. AD# B004159L.*

[4] *R. F. Benck, G. L. Filbey, Jr. and E. A. Murray, Jr., "Quasi-Static Compression Stress-Strain Curves--IV, 2024-T3510 and 6061-T6 Aluminum", BRL Memorandum Report 2655, Ballistic Research Laboratory, Aberdeen Proving Ground, MD, August 1976. AD #B013221L*

[5] *R. F. Benck and G. L. Filbey, Jr., "Elastic Constants of Aluminum Alloys, 2024-T3510, 5083-H131 and 7039-T64 as Measured by a Sonic Technique", BRL Memorandum Report 2649, Ballistic Research Laboratory, Aberdeen Proving Ground, MD, August 1976. AD #B012953L*

[6] *R. F. Benck and D. A. DiBerardo, "Quasi-Static Tensile Stress-Strain Curves--I, 2024-T3510 Aluminum Alloy", BRL Memorandum Report No. 2587, Ballistic Research Laboratory, Aberdeen Proving Ground, MD, February 1976. AD #B009639L*

[7] *R. F. Benck, "Quasi-Static Tensile Stress-Strain Curves--II, Rolled Homogeneous Armor", BRL Memorandum Report No. 2703, Ballistic Research Laboratory, Aberdeen Proving Ground, MD, November 1976. AD #B016015L*

[8] *G. E. Hauver, "The Alpha Phase Hugoniot of Rolled Homogeneous Armor", BRL Memorandum Report No. 2652, Ballistic Research Laboratory, Aberdeen Proving Ground, MD, August 1976. AD #B013009L*

II. EXPERIMENTAL PROCEDURES

A series of rapid loading tests, i.e., at strain rates of the order of 0.42 s^{-1}, were performed at 23°C using an Instron Universal Testing Machine. This instrument provides a maximum cross head speed of 50 cm per minute. 450 by 450mm slabs of RHA (MIL12560B) were cut from 38mm and 100mm thick plate stock with an acetylene cutting torch. Segments suitable for turning on a lathe were cut from the center portion of these slabs to eliminate edge effects. The test specimens were prepared with the axial lengths parallel to the rolling direction of the plate. A drawing of a typical tensile specimen is shown in Figure 1.

A. Strain Measurements.

Two dual element high deformation foil strain gages (MM Type EP-08-062TT-120) were affixed to each test sample to provide strain versus time history during loading. The gages were bonded to the specimens with M-Bond-200. The useful working range of a bonded strain gage is determined by the strain at which the bond fails. This is approximately five percent strain for M-Bond-200 adhesive. The gage resistance is nominally 120 ohms and the nominal gage factor is 2.03. One strain gage pair measured the axial strain, the second gage pair measured the circumferential strain. The two axially aligned gages are monitored separately; the two circumferential gages are connected in series and the series combination is recorded. The outputs of these strain gages were recorded on a Model 556 Tektronix oscilloscope. A model 184 Tektronix time mark generator was used for time calibration.

The entire strain history of the specimens is required. In tensile tests, the strain beyond the normal working range of the foil strain gages can be measured by a clip-on extensometer. The length of the specimens in the present studies was not sufficient to accommodate the available extensometer. The strain, however, was measured by noting the elongation between two fiducial or gage marks on the specimen. Photographic coverage of the specimens containing the fiducial marks were made during the tensile tests. The elongation between the reference marks was used to correlate the strain measurements with the tensile load. A compromise between speed of recording and adequate resolution was the determining cause for selecting the following procedure. A Red Lake Hycam, 16mm motion picture camera was operated at approximately 300 frames per second (fps). Two Quartz iodine lamps, two high intensity incandescent lamps and one flood lamp provided sufficient illumination to record at 300 fps. Even under these lighting conditions, the test specimens required special preparations for photographing.

The surface near the ends of each specimen was painted with zinc chromate; the paint provided good contrast, reduced reflected glare and presented a more suitable sample for photographing (Figure 1). Scratch lines were engraved within the painted area and on the bare metal surface. The scratches were filled with chalk to improve the photographic contrast.

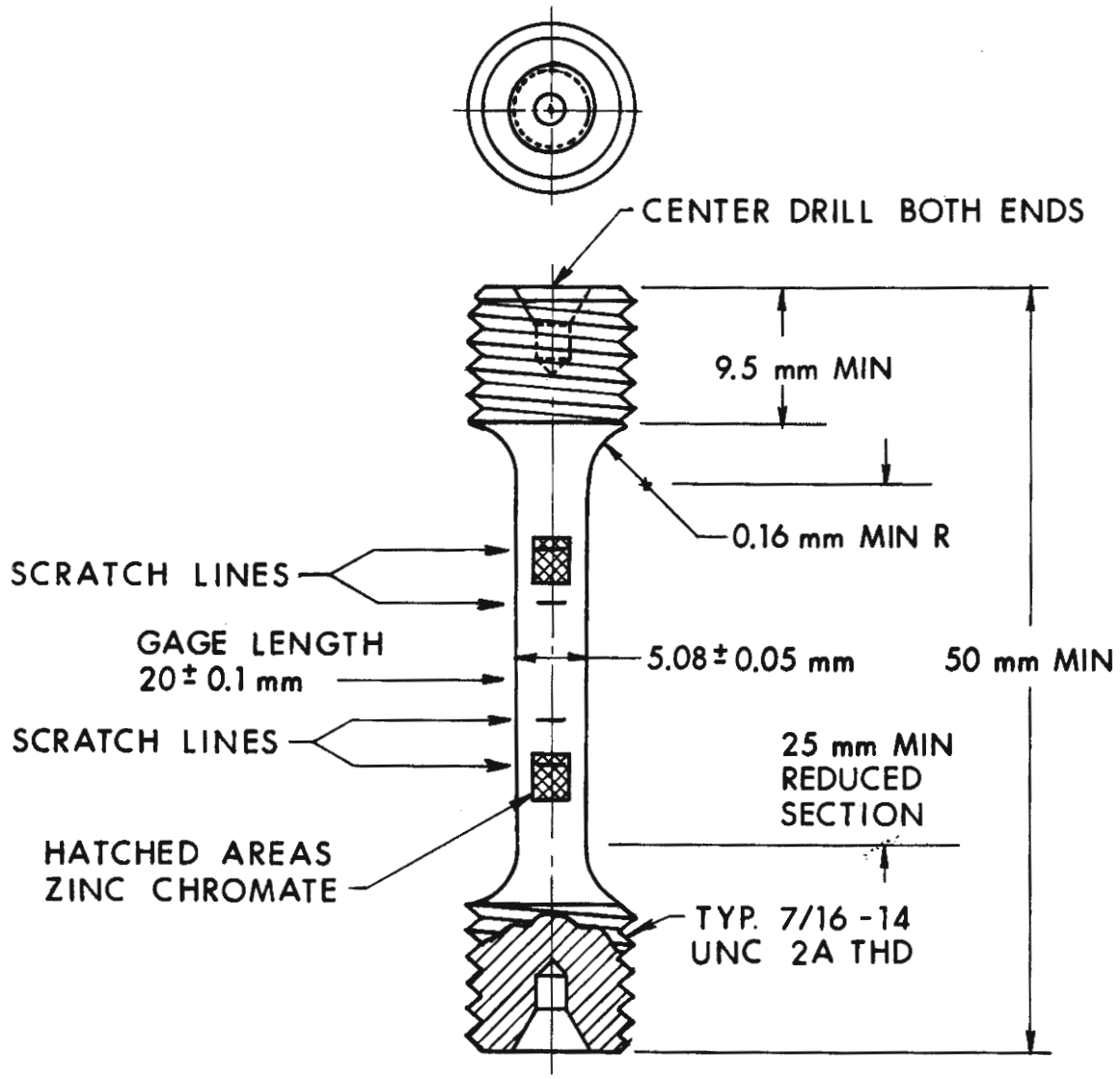

FIGURE 1: Typical RHA Tensile Specimen

GAF black and white reversal film, type 2962, with an ASA film rating 400 tungsten, provided the best quality image.

The camera has a built in triggering circuit which was used to trigger the monitoring oscilloscope and, to simultaneously light a 6-volt bulb. This triggering event was timed to occur when the camera speed reached a maximum. The lighting of the incandescent lamp signaled the operator to start the Instron instrument manually. Fiber optics were used to guide the light from the 6-volt bulb to the test setup to provide a time reference frame on the film. The time reference was used to determine actual loading time. The data collected from the Tektronix oscilloscope was correlated in time with the film recorded data.

A three-second full-scale stop watch with 0.01 second scale divisions was incorporated into the test setup and an image of the watch appeared in all frames of the film record. With the camera operating at 300 fps this technique provided times accurate to plus or minus three milliseconds. A picture of the experimental setup is shown in Figure 2, this picture is one frame taken from the photographic record of test 102.

After the test was completed, the film was developed and viewed with a standard film reader. A zero time was established with the lighting of the lamp. The framing speed of the camera was determined from the stop watch readings of the time period between load application and the occurrence of fracture.

Each specimen had scratches on both painted and unpainted portions of its surface. Only the scratch lines, however, within the painted area of the test specimen could be used to determine strain. The initial distance between the fiducial scratch marks are listed in Table I.

TABLE I

Initial Distance Between Scratch Marks
(Specimen Diameter is 20.3mm)

Test	Distance Between Fiducial Marks mm
98	6.470
100	5.028
101	4.493
102	4.670
103	5.229

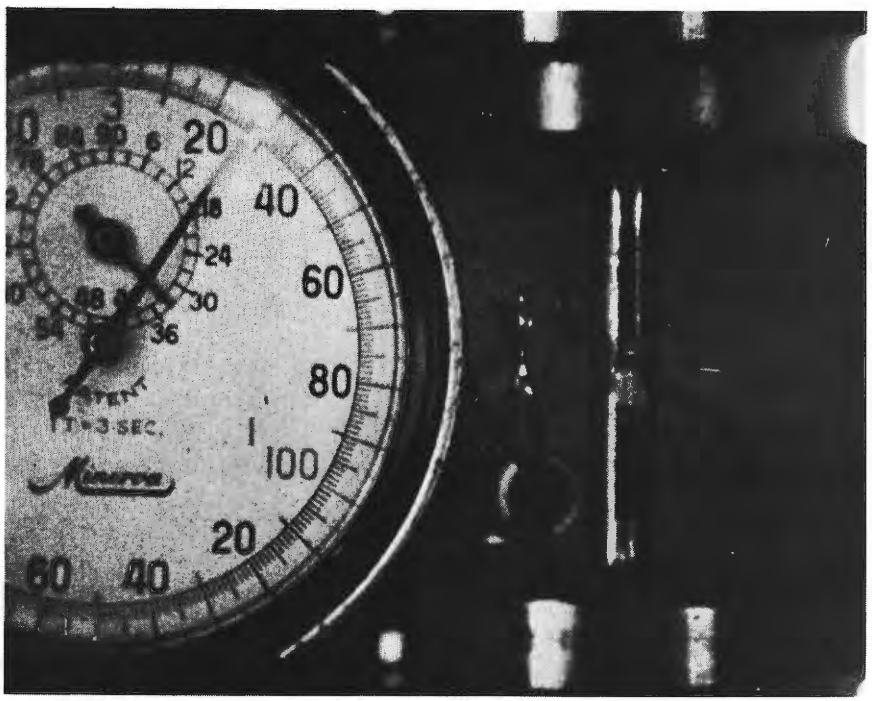

Figure 2: One Frame from the Photographic Record of Tensile Test 102.

B. Strain Corrections

The ASTM[9] has recommended that the gage length for a tensile test be four times that of the diameter of the specimen. Table I indicates that the gage lengths did not meet this criteria and therefore an expression for strain has been developed.[10] This expression is based on the assumption that after the specimen has reached its ultimate strength the only elongation taking place will be between the two fiducial marks.

Given:

L_o = initial gage length between fiducial marks used in experiment.

L_o' = any other initial gage length for which an equivalent strain at rupture is sought.

let $K = \frac{L_o'}{L_o}$

Until necking occurs, the strain is assumed to be uniform along the sample and is given by:

$$\varepsilon = \varepsilon' = \frac{L_o + (\Delta L_o - L_o)}{L_o} = \frac{\Delta L_o}{L_o} \qquad (1)$$

where ε = engineering strain as measured between the gage marks used.

ε' = engineering strain which would be measured between marks supplied by gage length L_o'.

ΔL_o = increase in length between fiducial marks used.

At the ultimate stress define

$$\Delta L_o \equiv \Delta L_E$$

ΔL_E = increase in distance between fiducial marks corresponding to stress increase from zero to its ultimate value.

---

[9] *ASTM Committee E-28 on Mechanical Testing, ANS Z165 13-1971, "Standard Methods of Tension Testing of Metallic Materials", American National Standards Institute, 1969.*

[10] *R. F. Benck and G. Silsby, BRL Memorandum Report in Preparation, "Quasi-Static Compression and Tensile Stress-Strain Curves, Ta-10W and Vascomax 300 Maraging Steel", Ballistic Research Laboratory, Aberdeen Proving Ground, MD.*

Beyond this point, necking is assumed to begin. Taking strain to be the unit elongation at a point, and unit elongation to be the average unit elongation between gage marks, the strain and unit elongation are no longer identical. There is very high strain in the necking area and little additional strain in the unnecked areas between the gage marks. Thus, different gage lengths result in different reported elongations. The unit elongation as seen by the fiducial marks would be equal to:

$$\varepsilon = \frac{\Delta L_E + \Delta L_N}{L_o} \tag{2}$$

where ΔL_N is the increase in distance between fiducial marks experienced during necking.

The equivalent unit elongation for marks initially separated by L_o' would be:

$$\varepsilon' = \frac{\Delta L_E' + \Delta L_N}{L_o'} = \frac{K\Delta L_E + \Delta L_N}{KL_o} \tag{3}$$

Solving for ΔL_N from (2) and substituting in equation (3) one obtains:

$$\varepsilon' = \frac{K-1}{K} \frac{\Delta L_E}{L_o} + \frac{\varepsilon}{K} \quad . \tag{4}$$

Therefore, by measuring the unit elongation between existing gage marks at the ultimate stress, one can infer the elongation that would be experienced between gage marks of a different length.

C. Stress Calculations.

The tensile load was measured with the aid of a load cell. The load cell used in the present tests has a load range of 0 - 10,000 kilograms. The load cell output was recorded in one channel of the oscilloscope used to record the output of the strain gages. The load cell was calibrated by placing 50 kilograms of precision weights on the testing machine and recording the output on the oscilloscope.

III. RESULTS

The modulus of elasticity, E, yield strength, Y, ultimate strength, U, and Poisson's ratio, γ, for the two RHA plate thicknesses are presented for the individual tests in Table II. Yield strength is defined as that stress at which the specimens deviated 0.2 percent from proportionality of stress to strain. Table II also contains the measured and corrected (expression 4) strain at fracture.

TABLE II

MATERIAL PROPERTIES AT 23°C OF 38 AND 100-mm RHA AT A TENSILE STRAIN RATE OF 0.42 s^{-1}

RHA Plate Thickness	38mm			100mm		
Test Number	98	100	102	99	101	103
Modulus of Elasticity, GPa	195	218	200	202	195	200
Yield Strength, MPa	840	830	820	715	710	690
Poisson's Ratio	0.25	0.30	0.32	0.29	0.26	0.27
Ultimate Strength, MPa	963	950	975	901	833	883
Reduction in Area, %	63	59	63	69	65	68
Measured Strain at Fracture, %	49	46	50	not measured	64	58
Strain at Fracture reduced to a gage length of 20mm, %	22	18	15	not measured	25	26

The individual data for the various tests are presented in Tables III and IV. The strains reported in Tables III and IV are longitudinal, which in the case of the foil gages are the averages of the two axial gages. The foil strain gage and stress data presented in Tables III and IV are the results of digitizing oscilloscope records. An example of such an oscillogram is shown in Figure 3 for test 103. The bottom trace is the load (calibrated at 500 kg per cm of deflection). The second from the bottom and top (inverted) traces are of the output of the two axial gages. The third from the bottom trace is the average of the series connected circumferential gages (1 cm deflection was calibrated to be 2.5 percent strain). Time marks are at 0.1 s intervals.

Stress-strain data were obtained by combining the photographic records of strain-time with the oscilloscopic recorded loads. An example of a strain-time curve is presented in Figure 4. These strain-time curves showed a considerable amount of scatter and to maximize their usefulness a smooth curve was drawn through the data points. It is from these smooth curves that the camera strain data shown in Tables III and IV were taken.

TABLE III

STRESS-STRAIN VALUES FOR THE INDIVIDUAL TESTS OF 38mm RHA

Test 98				Test 100			
Foil Strain Gages		Camera		Foil Strain Gages		Camera	
Stress MPa	Strain %	Stress MPa	Strain %	Stress MPa	Strain %	Stress MPa	Strain %
0	0	0	0	0	0	908	4.38
		910	2.00	200	0.020	920	5.00
90	0.020	915	2.50	402	0.050	930	5.56
117	0.025	925	2.75	597	0.113	938	5.94
173	0.037	944	3.75	655	0.138	940	6.56
200	0.042	948	4.75	733	0.175	942	7.19
236	0.050	951	5.25	765	0.225	950	8.50
297	0.055	955	6.00	781	0.363	952	9.31
357	0.075	959	7.75	799	0.563	948	10.00
415	0.095	962	9.00	812	0.813	942	11.00
474	0.105	958	10.50	822	1.338	940	11.88
530	0.120	956	12.00	832	1.612	932	12.81
590	0.150	950	14.00	842	1.962	920	14.38
636	0.177	935	17.50	850	2.200	912	15.75
705	0.213	892	23.50	860	2.438	900	17.38
746	0.250	870	25.70	870	2.689	890	18.75
780	0.290	861	27.00	878	2.850	875	20.63
810	0.375	842	29.50	884	3.013	866	22.15
835	0.450	832	30.75	890	3.263	846	25.31
844	0.535	820	32.00	894	3.588	839	27.06
860	0.613	807	33.25	896	3.763	832	28.75
870	0.788	795	34.50	900	4.000	810	30.63
880	0 975	785	35.70	902	4.213	800	32.50
890	1.200	772	37.00	905	4.388	785	34.69
989	1.500	762	38.25	906	4.612	775	36.25
904	1.625	726	42.00	907	4.825	752	38.75
910	1.750	712	43.75	908	5.038	740	40.63
917	1.925	703	45.00			732	42.50
922	2.050	685	46.50			705	45.63
926	2.150	670	47.25				
		655	49.25				

TABLE III (CONT'D)

Test 102			
Foil Strain Gages		Camera	
Stress MPa	Strain %	Stress MPa	Strain %
0	0		
29	0.020	0	0
51	0.033	700	0.31
75	0.035	850	0.40
152	0.040	885	0.63
240	0.078	915	0.75
305	0.108	930	0.94
355	0.150	955	1.69
430	0.200	960	1.88
520	0.252	965	2.19
580	0.307	968	2.50
650	0.355	972	2.63
751	0.420	978	3.19
793	0.545	979	3.75
854	0.758	980	4.38
893	1.125	980	4.88
912	1.540	980	5.31
927	1.860	980	5.50
951	2.257	980	6.25
959	2.630	980	6.88
963	2.970	976	7.50
967	3.300	972	8.13
971	3.480	965	8.94
974	3.860	960	10.00
978	4.060	951	10.94
		945	11.88
		935	13.00
		920	14.38
		910	16.25
		900	17.81
		887	19.38
		880	20.94
		870	22.50
		850	24.38
		830	25.63
		815	27.50

TABLE IV

STRESS-STRAIN VALUES FOR INDIVIDUAL TESTS OF 100mm RHA

Test 99*		Test 101					
Foil Strain Gages		Foil Strain Gages		Camera		Camera (Cont'd)	
Stress MPa	Strain %	Stress MPa	Strain %	Stress MPa	Strain %	Stress MPa	Strain %
		0	0	0	0		
0	0	150	.08	375	0.01	817	19.05
175	0.038	183	.10	502	0.10	813	19.81
210	0.050	250	.14	562	0.30	808	20.56
290	0.125	316	.17	622	0.60	802	21.17
400	0.150	361	.21	652	0.85	799	22.07
460	0.188	423	.23	671	1.06	791	22.98
560	0.225	500	.26	691	1.33	787	23.58
620	0.263	564	.35	709	1.63	776	24.95
645	0.313	616	.55	716	1.96	769	26.00
675	0.400	636	.68	727	2.27	759	27.21
705	0.488	652	.94	739	2.60	752	28.42
720	0.625	663	1.22	748	3.02	743	29.63
735	0.875	675	1.41	757	3.33	735	31.14
750	1.125	688	1.62	769	3.63	728	32.50
765	1.300	699	1.80	775	4.23	720	34.17
780	1.500	706	2.00	781	4.54	712	35.68
788	1.700	714	2.21	787	4.99	700	37.19
800	1.875	720	2.45	793	5.44	690	39.31
815	2.350	729	2.61	799	5.90	679	41.73
830	2.750	735	2.71	804	6.50	664	42.94
848	3.375	744	2.92	808	6.96	652	45.04
860	4.200	750	3.16	810	7.56	638	47.17
877	4.900	757	3.31	811	8.01	625	49.59
888	5.600	762	3.54	814	8.62	615	52.01
892	6.000	768	3.87	817	9.07	604	54.43
899	7.100	772	4.06	817	9.83	585	57.75
900	7.700	777	4.31	819	10.28	562	60.48
901	8.100	778	4.57	821	10.89	540	63.80
902	8.510	784	4.76	823	11.64		
		787	5.03	826	12.25		
		790	5.30	829	12.85		
		793	5.47	831	13.61		
		795	5.72	832	14.21		
		798	5.91	831	14.82		
		799	6.01	829	15.42		
		801	6.20	828	16.18		
		802	6.41	826	16.93		
		804	6.76	825	17.69		
		806	7.01	821	18.44		

*The camera failed for this test and therefore there is only foil strain gage data available.

TABLE IV (CONT'D)

Test 103			
Foil Strain Gages		Camera	
Stress MPa	Strain %	Stress MPa	Strain %
0	0	0	0
26	0.015	246	0.10
127	0.020	454	0.36
416	0.025	525	0.73
450	0.050	602	1.09
551	0.125	656	1.45
615	0.150	687	1.81
634	0.225	700	2.17
658	0.255	717	2.55
695	0.450	733	2.90
713	0.700	749	3.26
756	1.310	766	3.62
759	1.670	780	3.99
767	2.950	813	5.75
772	3.300	848	7.56
775	3.570	863	9.37
778	3.750	870	11.18
785	3.900	878	13.00
788	4.125	883	14.81
793	4.350	878	16.62
794	4.450	871	18.43
		859	20.24
		848	22.05
		823	25.67
		815	27.49
		799	29.30
		790	31.11
		771	32.92
		756	34.73
		733	36.55
		727	38.36
		718	40.17
		695	41.98
		660	45.60
		645	47.42
		634	49.23
		623	51.04
		591	54.66
		536	58.65

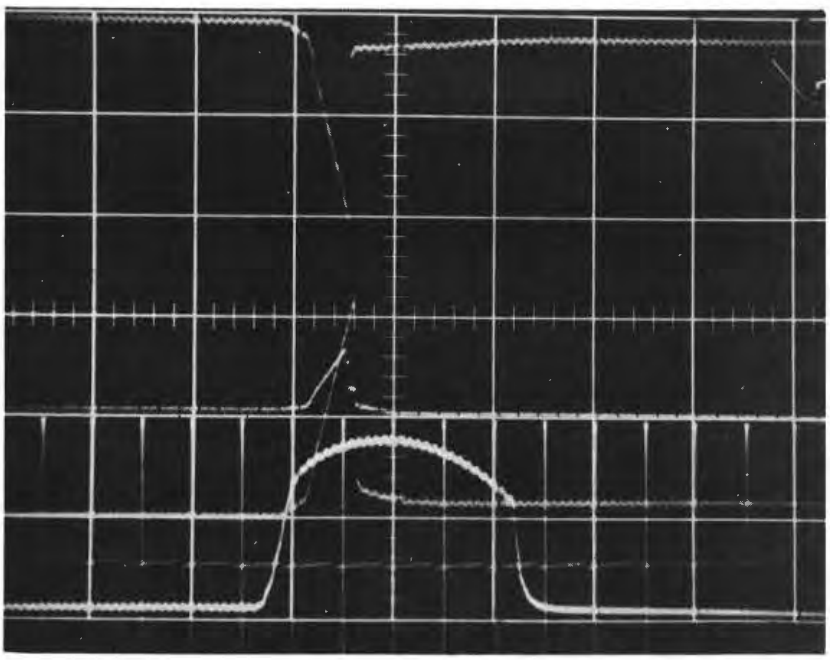

Figure 3: Oscillogram of Test 103, the traces are: Bottom to Top; (1) load cell, (2) axial gage #2, (3) circumferential gages and (4) axial gage #1 (inverted). 0.1 s time marks.

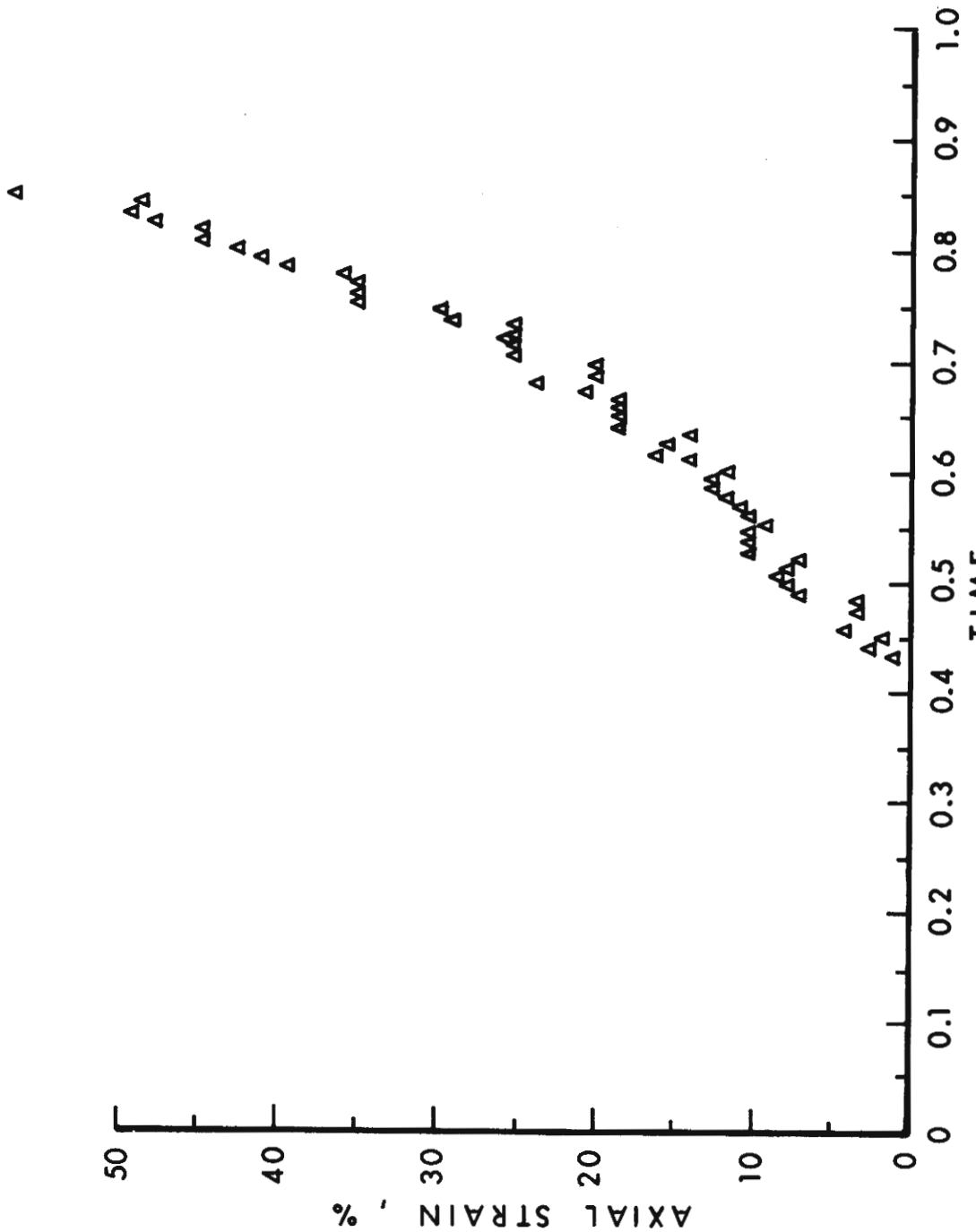

Figure 4: Axial strain (as calculated from the camera recorded specimen elongation) versus time for Test 103.

Engineering stress versus engineering strain curves for the 38mm and 100mm RHA plates are presented in Figures 5 and 6, respectively.

Figure 7 is a photograph of specimens 99 and 100 after fracture. The fracture surface appeared as a cup and cone and did not always occur at the midpoint; a fact which necessitated the use of a series of scribe marks. The average material properties of 38 and 100mm thick RHA plate at strain rates of 0.42 and 3×10^{-4} s^{-1} are presented in Table V. The values for hardness shown in Table V are averages taken across the thickness of the original RHA samples.[8]

TABLE V

EFFECT OF STRAIN RATE ON MATERIAL PROPERTIES OF 38 AND 100-mm RHA AT 23°C

	38mm RHA Plate		100mm RHA Plate	
Strain Rate, s^{-1}	3×10^{-4} [7]	0.42	3×10^{-4} [7]	0.42
Hardness[8], Rockwell "C"	30-31	30-31	27	27
E, GPa	204.8	204.3	206.9	199.1
γ	0.27	0.29	0.27	0.27
Y, MPa	821	830	701	705
U, MPa	933	963	862	872
Strain at Fracture, %	18.8	18.[a]	21.9	25.[a]

[a]Corrected strain for gage length equal to four diameters.

IV. DISCUSSION

The data in Table V indicate that varying the strain rate from 3×10^{-4} to 0.42 s^{-1} will not effect the material properties of the RHA tested. There is a slight increase in the yield and ultimate strengths for the faster tests, however the amount of increase is probably within the experimental accuracy of the tests.

The data for the 0.42 s^{-1} tests are not as precise as that obtained in lower strain rate tests. The uncertainty in precision is still probably no worse than plus or minus one to two percent. Errors associated with digitizing the oscillograph records typically are in the order of plus or minus 0.25 MPa in stress and plus or minus 0.005 percent in strain.

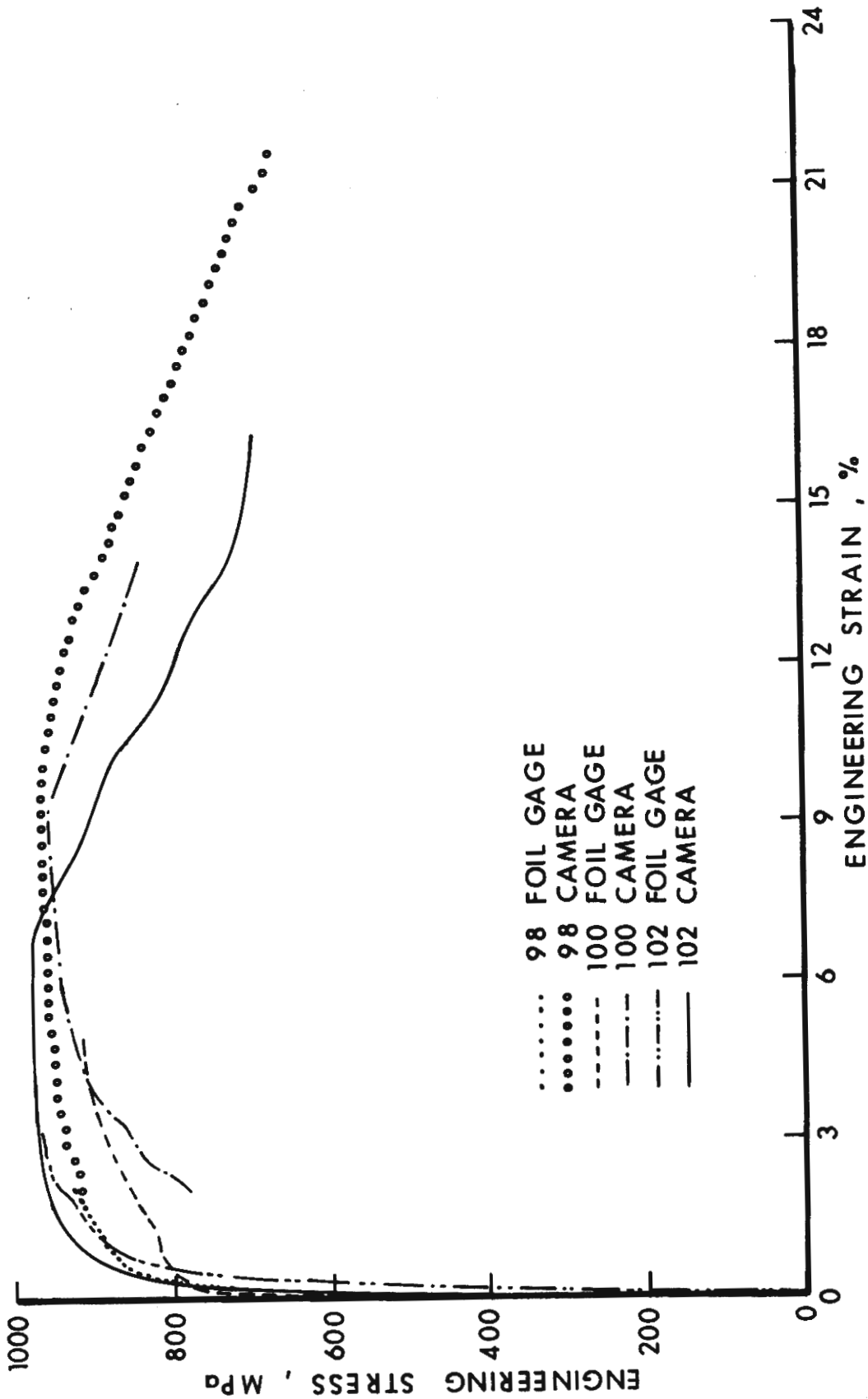

Figure 5: Engineering stress versus engineering strain for 38mm RHA plate, Tests 98, 100, and 102.

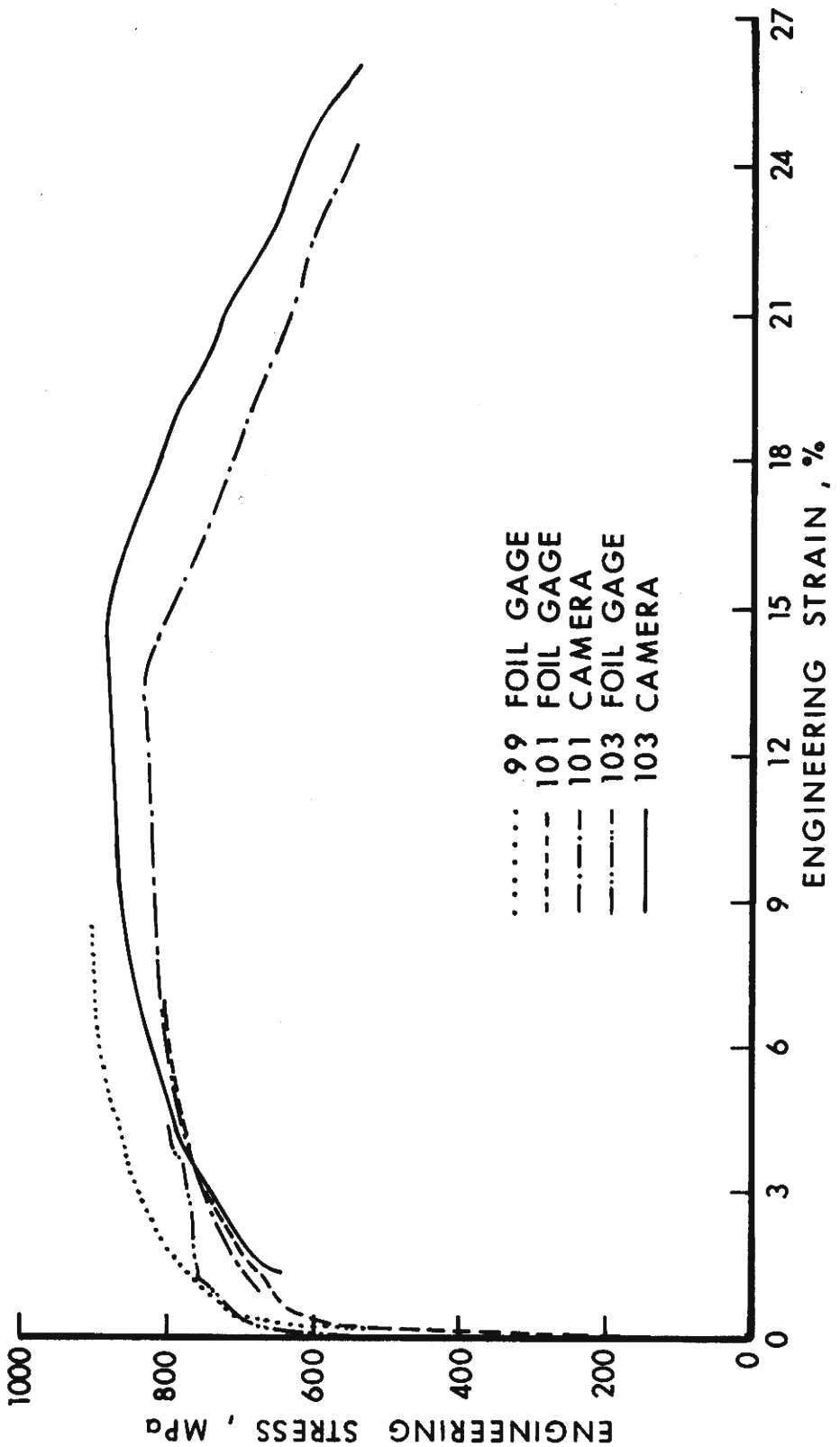

Figure 6: Engineering stress versus engineering strain for 100mm RHA plate, Tests 99, 101, and 103.

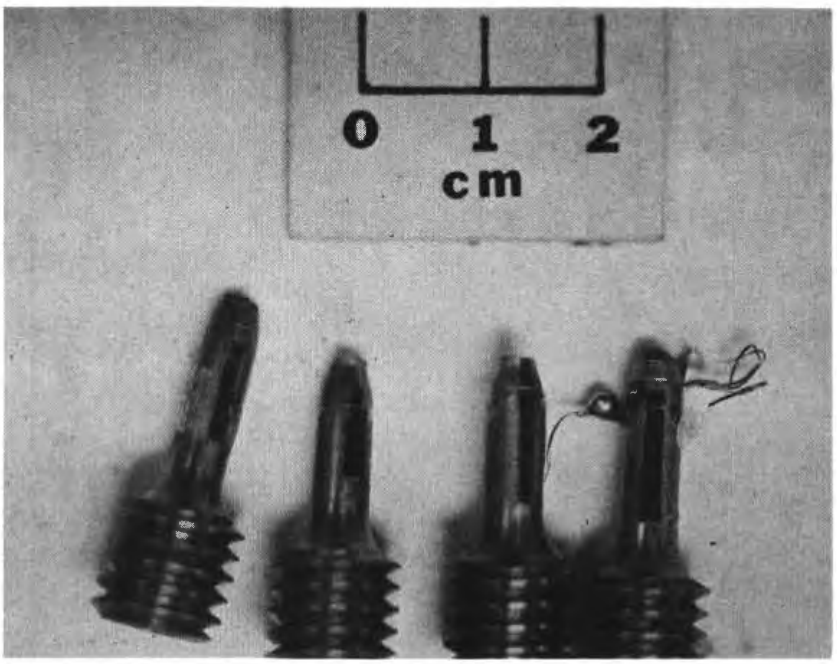

Figure 7: Post fracture photographs of specimens 99 and 100.

The error in reading the film to determine the sample elongation is probably plus or minus one percent. The largest source of error in constructing the stress-strain curves is probably in correlating the elongation with time and hence with load or stress. The least reliable camera data are at low strains. The "best" total stress-strain curve is obtained by using the foil strain gage data to gage failure and then the elongation (camera) strain to specimen fracture.

Interpretation of stress-strain data is usually straightforward up to the strain at ultimate load. Until the ultimate load is reached, the specimen elongates uniformly. Once the ultimate load is reached, the specimen starts to neck, that is, the strain is no longer uniform along the specimen. One of the better ways to present stress-strain data beyond the onset of necking is through a true stress-true strain relationship[11]. True stress involves knowing the actual cross-sectional area of the specimen at the time of strain measurement. In the present study, since we do have a series of specimen photographs taken during the tensile test, we hoped to measure the specimen diameter as a function of elongation and to construct true stress-true strain curves. Unfortunately, as the specimens were being pulled, the foil strain gages became unbonded and obscured the camera view of the specimen diameter. The strains beyond ultimate stress have been referred to a common gage length (four specimen diameters) so that they can be compared to reported values such as Reference 7.

V. CONCLUSIONS

Young's modulus, Poisson's ratio, yield and ultimate strengths of 38 and 100mm thick RHA steel, sampled in an orientation parallel to the rolling direction of the plates, have been measured at a strain rate of 0.42 s^{-1}.

The results indicate that there is a very slight (<5 percent) increase in yield and ultimate strengths as compared to tests performed at strain rates of 3 x 10^{-4} s^{-1}.

---

[11] *A. Nadai, "Theory of Flow and Fracture of Solids", McGraw-Hill Book Co., Inc., New York, N.Y., 1950, pp. 7089.*

REFERENCES

1. E. A. Murray, Jr. and J. H. Suckling, "Quasi-Static Compression Stress-Strain Curves--I, Data Gathering and Reduction Procedures; Results for 1066 Steel", BRL Memorandum Report No. 2399, Ballistic Research Laboratory, Aberdeen Proving Ground, MD, January 1974. AD# 922704L.

2. E. A. Murray, Jr., "Quasi-Static Compression Stress-Strain Curves--II, 7039-T64 Aluminum", BRL Memorandum Report No. 2589, Ballistic Research Laboratory, Aberdeen Proving Ground, MD, February 1976. AD #B009646L

3. R. F. Benck and E. A Murray, Jr., "Quasi-Static Compression Stress-Strain Curves--III, 5083-H131 Aluminum", BRL Memorandum Report No. 2480, Ballistic Research Laboratory, Aberdeen Proving Ground, MD, May 1975. AD# B004159L.

4. R. F. Benck, F. L. Filbey, Jr. and E. A. Murray, Jr., "Quasi-Static Compression Stress-Strain Curves--IV, 2024-T3510 and 6061-T6 Aluminum", BRL Memorandum Report 2655, Ballistic Research Laboratory, Aberdeen Proving Ground, MD, August 1976. AD #B013221L

5. R. F. Benck and G. L. Filbey, Jr., "Elastic Constants of Aluminum Alloys, 2024-T3510, 5083-H131 and 7039-T64 as Measured by a Sonic Technique", BRL Memorandum Report 2649, Ballistic Research Laboratory, Aberdeen Proving Ground, MD, August 1976. AD #B012953L

6. R. F. Benck and D. A. DiBerardo, "Quasi-Static Tensile Stress-Strain Curves--I, 2024-T3510 Aluminum Alloy", BRL Memorandum Report No. 2587, Ballistic Research Laboratory, Aberdeen Proving Ground, MD, February 1976. AD #B009639L

7. R. F. Benck, "Quasi-Static Tensile Stress-Strain Curves--II, Rolled Homogeneous Armor", BRL Memorandum Report No. 2703, Ballistic Research Laboratory, Aberdeen Proving Ground, MD, November 1976. AD #B016015L

8. G. E. Hauver, "The Alpha Phase Hugoniot of Rolled Homogeneous Armor", BRL Memorandum Report No. 2652, Ballistic Research Laboratory, Aberdeen Proving Ground, MD, August 1976. AD #B013009L

9. ASTM Committee E-28 on Mechanical Testing, ANS Z165 13-1971, "Standard Methods of Tension Testing of Metallic Materials", American National Standards Institute, 1969.

10. R. F. Benck and G. Silsby, BRL Memorandum Report in Preparation, "Quasi-Static Compression and Tensile Stress-Strain Curves, Ta-10W and Vascomax 300 Maraging Steel", Ballistic Research Laboratory, Aberdeen Proving Ground, MD.

11. A. Nadai, "Theory of Flow and Fracture of Solids", McGraw-Hill Book Co., Inc., New York, N.Y., 1950, pp. 70-89.

DISTRIBUTION LIST

No. of Copies	Organization
12	Commander Defense Documentation Center ATTN: DDC-TCA Cameron Station Alexandria, VA 22314
1	Director Defense Advanced Research Projects Agency ATTN: Tech Info 1400 Wilson Boulevard Arlington, VA 22209
1	Commander US Army Materiel Development and Readiness Command ATTN: DRCDMA-ST 5001 Eisenhower Avenue Alexandria, VA 22333
1	Commander US Army Materiel Development and Readiness Command ATTN: DRCDLDL 5001 Eisenhower Avenue Alexandria, VA 22333
1	Commander US Army Aviation Systems Command ATTN: DRSAV-E 12th and Spruce Streets St. Louis, MO 63166
1	Director US Army Air Mobility Research and Development Laboratory Ames Research Center Moffett Field, CA 94035
2	Commander US Army Electronics Command ATTN: DRSEL-RD DRSEL-HL-CT, S.Crossman Fort Monmouth, NJ 07703
2	Commander US Army Missile Research and Development Command ATTN: DRDMI-R DRDMI-RBL Redstone Arsenal, AL 35809
1	Commander US Army Tank Automotive Development Command ATTN: DRDTA-RWL Warren, MI 48090
2	Commander US Army Mobility Equipment Research & Development Command ATTN: Tech Docu Cen, Bldg. 315 DRSME-RZT Fort Belvoir, VA 22060
1	Commander US Army Armament Materiel Readiness Command Rock Island, IL 61202
1	Commander US Army Electronic Proving Ground ATTN: Tech Lib Fort Huachuca, AZ 85613
1	Commander US Army Watervliet Arsenal ATTN: Dr. F. Schneider Watervliet, NY 12189
1	Commander US Army Harry Diamond Labs ATTN: DRXDO-TI 2800 Powder Mill Road Adelphi, MA 20783
1	Commander US Army Natick Research and Development Center ATTN: DRXRE, Dr. D. Sieling Natick, MD 01762

DISTRIBUTION LIST

No. of Copies	Organization
5	Commander US Army Materials and Mechanics Research Center ATTN: DRXMR-ATL DRXMR-T, J. Bluhm DRXMR-XH, J. Dignam DRXMR-XO, E. Hagge DRXMR-XP, Dr. J. Burke Watertown, MA 02172
1	Director US Army TRADOC Systems Analysis Activity ATTN: ATAA-SA White Sands Missile Range NM 88002
1	Deputy Assistant Secretary of the Army (R&D) Department of the Army Washington, DC 20310
1	HQDA (DAMA-ARP-P, Dr. Watson) Washington, DC 20310
1	HQDA (DAMA-MS) Washington, DC 20310
1	Commander US Army Research Office P. O. Box 12211 Research Triangle Park NC 27709
1	Commander US Army Ballistic Missile Defense Systems Command ATTN: SENSC, Mr. Davidson P. O. Box 1500 Huntsville, AL 35804
1	Director US Army Advanced BMD Technology Center ATTN: CRDABH-5, W. Loomis P. O. Box 1500, West Station Huntsville, AL 35807
1	Commander US Army War College ATTN: Lib Carlisle Barracks, PA 17013
1	Commander US Army Command and General Staff College ATTN: Archives Fort Leavenworth, KS 66027
1	Mathematics Research Center US Army University of Wisconsin Madison, WI 53706
3	Commander US Naval Air Systems Command ATTN: AIR-604 Washington, DC 20360
3	Commander US Naval Ordnance Systems Command ATTN: ORD-0632 ORD-035 ORD-5524 Washington, DC 20360
1	Office of Naval Research Department of the Navy ATTN: Code 402 Washington, DC 20360
1	Commander US Naval Surface Weapons Center ATTN: Code Gr-9, Dr. W. Soper Dahlgren, VA 22448

DISTRIBUTION LIST

No. of Copies	Organization
1	Commander and Director US Naval Electronics Laboratory ATTN: Lib San Diego, CA 92152
3	Commander US Naval Research Laboratory ATTN: Code 5270, F. MacDonald Code 2020, Tech Lib Code 7786, J. Baker Washington, DC 20375
1	AFATL (DLYW) Eglin AFB, FL 32542
1	AFATL (DLDG) Eglin AFB, FL 32542
1	AFATL (DLDL, MAJ J. E. Morgan) Eglin AFB, FL 32542
1	RADC (EMTLD, Lib) Griffiss AFB, NY 13440
1	AUL (3T-AUL-60-118) Maxwell AFB, AL 36112
1	AFFDL/FB, Dr. J. Halpin Wright-Patterson AFB, OH 45433
1	Director Environmental Science Service Administration US Department of Commerce Boulder, CO 80302
1	Director Jet Propulsion Laboratory ATTN: Lib (TDS) 4800 Oak Grove Drive Pasadena, CA 91103
1	Director National Aeronautics and Space Administration Manned Spacecraft Center ATTN: Lib Houston, TX 77058
1	Dupont Experimental Labs ATTN: Mr. J. Lupton Wilmington, DE 19801
7	Sandia Laboratories ATTN: Mr. L. Davison Div 5163 Dr. C. Harness H. J. Sutherland Code 5133 Code 1721 Dr. P. Chen Albuquerque, NM 87115
5	Brown University Division of Engineering ATTN: Prof. R. Clifton Prof. H. Kolsky Prof. A. Pipkin Prof. P. Symonds Prof. J. Martin Providence, RI 02192
5	California Institute of Technology Division of Engineering and Applied Science ATTN: Dr. J. Milowitz Dr. E. Sternberg Dr. J. Knowles Dr. T. Coguhey Dr. R. Shield Pasadena, CA 91102

DISTRIBUTION LIST

No. of Copies	Organization
4	Carnegie Mellon University Department of Mathematics ATTN: Dr. D. Owen Dr. M. E. Gurtin Dr. B. Coleman Dr. W. Williams Pittsburgh, PA 15213
2	Catholic University of America School of Engineering and Architecture ATTN: Prof. A. Durelli Prof. J. McCoy Washington, DC 20017
1	Harvard University Division of Engineering and Applied Physics ATTN: Dr. G. Carrier Cambridge, MA 02138
2	Iowa State University Engineering Research Lab. ATTN: Dr. G. Nariboli Dr. A. Sedov Ames, IA 50010
3	Lehigh University Center for the Application of Mathematics ATTN: Dr. E. Varley Dr. R. Rivlin Prof. M. Mortell Bethlehem, PA 18015
1	Massachusetts Institute of Technology ATTN: Dr. R. Probstein 77 Massachusetts Avenue Cambridge, MA 02139
1	Michigan State University College of Engineering ATTN: Prof. W. Sharpe East Lansing, MI 48823
1	New York University Department of Mathematics ATTN: Dr. J. Keller University Heights New York, NY 10053
1	North Carolina State University Department of Engineering Mechanics ATTN: Dr. W. Bingham P. O. Box 5071 Raleigh, NC 27607
2	Pennsylvania State University Engineering Mechanical Dept. ATTN: Dr. R. M. Haythornthwaite Prof. N. Davids University Park, PA 16802
2	Forrestal Research Center Aeronautical Engineering Lab. Princeton University ATTN: Dr. S. Lam Dr. A. Eringen Princeton, NJ 08540
1	Purdue University Institute for Mathematical Sciences ATTN: Dr. E. Cumberbatch Lafayette, IN 47907
2	Rice University ATTN: Dr. R. Bowen Dr. C. C. Wang P. O. Box 1892 Houston, TX 77001
1	Southern Methodist University Solid Mechanics Division ATTN: Prof. H. Watson Dallas, TX 75221

DISTRIBUTION LIST

No. of Copies	Organization
2	Southwest Research Institute Department of Mechanical Sciences ATTN: Dr. U. Lindholm Dr. W. Baker 8500 Culebra Road San Antonio, TX 78228
1	Tulane University Dept of Mechanical Engineering ATTN: Dr. S. Cowin New Orleans, LA 70112
2	University of California ATTN: Dr. M. Carroll Dr. P. Naghdi Berkeley, CA 94704
1	University of California Dept of Aerospace and Mechanical Engineering Science ATTN: Dr. Y. C. Fung P. O. Box 109 La Jolla, CA 92037
1	University of California Department of Mechanics ATTN: Dr. R. Stern 504 Hilgard Avenue Los Angeles, CA 90024
1	University of Delaware Department of Mechanical Engineering ATTN: Prof. J. Vinson Newark, DE 19711
3	University of Florida Dept of Engineering Science and Mechanics ATTN: Dr. C. A. Sciammarilla Dr. L. Malvern Dr. E. Walsh Gainesville, FL 32601
2	University of Houston Department of Mechanical Engineering ATTN: Dr. T. Wheeler Dr. R. Nachlinger Houston, TX 77004
1	University of Illinois Dept of Theoretical and Applied Mechanics ATTN: Dr. D. Carlson Urbana, IL 61801
2	University of Illinois at Chicago Circle College of Engineering Dept of Materials Engineering ATTN: Prof. A. Schulta Dr. T. C. T. Ting P. O. Box 4348 Chicago, IL 60680
1	University of Iowa ATTN: Dr. L. Valanis Iowa City, IA 52240
4	University of Kentucky Dept of Engineering Mechanics ATTN: Dr. M. Beatty Prof. O. Dillon, Jr. Prof. P. Gillis Dr. D. Leigh Lexington, KY 40506
2	The University of Maryland Department of Mechanical Engineering ATTN: Prof. J. Yang Dr. J. Dally College Park, MD 20742
1	University of Minnesota Dept of Engineering Mechanics ATTN: Dr. R. Fosdick Minneapolis, MN 55455

DISTRIBUTION LIST

No. of Copies	Organization
1	University of Notre Dame Department of Metallurgical Engineering and Materials Sciences ATTN: Dr. N. Fiore Notre Dame, IN 46556
1	University of Pennsylvania Towne School of Civil and Mechanical Engineering ATTN: Prof. Z. Hashin Philadelphia, PA 19105
4	University of Texas Department of Engineering Mechanics ATTN: Prof. H. Calvit Dr. M. Stern Dr. M. Bedford Prof. Ripperger Austin, TX 78712
1	University of Washington Department of Mechanical Engineering ATTN: Prof. J. Chalupnik Seattle, WA 98105
2	Yale University ATTN: Dr. B. Chu Dr. E. Onat 400 Temple Street New Haven, CT 96520
	Aberdeen Proving Ground
	Marine Corps Ln Ofc Dir, USAMSAA